# Intestinal Epithelial Restitution

## Characterization of a Cell Culture Model and Mapping of Cytoskeletal Elements in Migrating Cells

**Asma Nusrat, Charlene Delp, and James L. Madara**
*Departments of Pathology, Brigham and Women's Hospital and Harvard Medical School, and the Harvard Digestive Diseases Center, Boston, Massachusetts 02115*

## Abstract

**Closure of superficial wounds in epithelia occurs by migration of cells shouldering the wound. We describe an in vitro model of such restitution using a human intestinal epithelial cell line, T84. T84 cells were grown on novel optically transparent type 1 collagen membranes without underlying filter supports. Monolayers so grown display substantial barrier function (400–500 ohm · $cm^2$; 1.3±0.4 nmol · $h^{-1}$ · $cm^{-2}$ mannitol flux). Wounds made with micropipettes were accompanied by a fall in resistance and rise in monolayer permeability to mannitol and inulin. After injury, cells shouldering wounds migrated, by extension of lamellipodia-like processes, to reseal wounds as defined by structural and functional criteria. F actin arcs crossed the base of the lamellipodia-like extensions and F actin microspikes projected from the leading edge of these extensions. Villin, an epithelial-specific cytoskeletal protein with both F actin bundling and severing capacities, was also expressed at the leading edge in a pattern consistent with a regulatory role in the dynamic restructuring of lamellipodia. Lastly, myosin II was predominantly localized to the basal regions of lamellipodia, though occasional staining was seen close to the advancing edge. Myosin I, a recently recognized myosin family member considered to be essential for fibroblast and slime mold motility, was present throughout lamellipodia in punctate fashion, but was not concentrated at the leading edge. (*J. Clin. Invest.* 1992. 89:1501–1511.) Key words: cytoskeleton • villin • myosin • wound healing**

## Introduction

The epithelial lining of the alimentary tract forms an important barrier to a wide array of noxious substances in the lumen. Rapid resealing of injuries to this barrier is thus of major physiological importance. This key barrier has a striking capacity for resealing superficial wounds, a process that is termed restitution and occurs both in vitro (1–3) and in vivo (3) throughout the alimentary tract and in related columnar epithelia. Restitution refers to resealing of superficial wounds occurring as a consequence of epithelial cell migration into the defect, rather than of epithelial cell proliferation. Other events, such as contraction of underlying fibroblasts, may also contribute to restitution (4). The restitution process is particularly remarkable, for it necessitates that differentiated polarized columnar epithelial cells flatten, spread, migrate, and ultimately repolarize. Motility of cells such as fibroblasts and macrophages has been investigated in detail (5, 6, see reference 7 for review). The mechanisms by which polarized epithelial cells change to the flattened phenotype and become motile is not as extensively characterized. Study of such events during epithelial motility is severely limited in natural mucosae, due to their complex geometry, heterogeneity, and finite in vitro life span. In contrast, cultured cell lines do not have such limitations. The T84 polarized human intestinal epithelial cell line with many cytoskeletal and junctional features similar to those of natural intestinal epithelia (8–10) forms electrically tight monolayers. For this reason, we have utilized this cell as a model to better characterize migration events during restitution. As will be detailed, the wounded edges of T84 monolayers recapitulate the general structural features occurring at intestinal wound margins during restitution. In this in vitro model, such features can be studied with ease and in substantially greater detail. Also, as will be shown, these cells exhibit several general features of motility shared by nontransformed cells (macrophages, fibroblasts) during migration. We also define a model of restitution in which motile epithelial cells can be easily visualized. T84 cells are grown on optically clear collagen sheets assembled onto polycarbonate rings without underlying filter supports that interfere with visualization. Using such a model, highly defined wounds can be made in monolayers without disturbing the underlying matrix. This is achieved by suction through a micropipette applied to the surface of a small disk of T84 cells. Such preparations permit continuous studies of both cell morphology and physiological events during restitution, and allow us to define cytoskeletal specializations at such sites. For example, we show that F actin and an actin-regulating protein, villin, distribute to the leading edge, and that a recently recognized member of the myosin family, myosin I, thought to be important to motility in nonepithelial cells, is also expressed at the leading edge.

## Methods

### *Cell culture*

The T84 human colonic cell line (9, 11) was grown and passaged as previously described (11, 12). T84 monolayers were prepared on permeable supports of rat tail collagen, described below, or on glass coverslips.

### *Construction of permeable supports and monolayers*

T84 cells were grown as monolayers on translucent permeable supports of rat tail collagen in a culture dish constructed by a modification of that described by Steele (13). Type 1 collagen was extracted from rat tail tendons in 1% acetic acid using the method of Cerijido (14). We found that commercially available type 1 collagen preparations do not pro-

Address correspondence and reprint requests to Dr. Asma Nusrat, Department of Pathology, Brigham and Women's Hospital, 20 Shattuck Street-Room 1423, Boston, MA 02115.

*Received for publication 28 June 1991 and in revised form 20 November 1991.*

J. Clin. Invest.

0021-9738/92/05/1501/11 $2.00
Volume 89, May 1992, 1501–1511

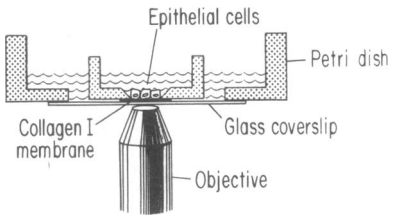


*Figure 1.* Chamber design used to study restitution of T84 monolayers in response to wounding. Translucent type 1 collagen membrane support made from rat tail collagen was attached to a polycarbonate ring and T84 cells plated at high density on this matrix to form monolayers. For imaging, the ring was placed in a glass-bottomed petri dish. Monolayers could be directly imaged or transferred to Ussing chambers modified for cell culture, or to sterile chamber devices for functional studies.

duce an optically clear substrate, presumably due to uniformity in collagen fibril size, and, hence, production of more uniformly packed, less hydrated, and therefore more light scattering crosslinked gel. Viscous collagen, isolated as above, was maintained at 4°C and was precleared by centrifugation at 25,000 *g* for ~ 30 min. This resulting collagen solution was applied to washed and boiled glass plates at 280 $\mu l/cm^{-2}$ and allowed to dry. The plate was then flooded with 3.5% ammonium hydroxide for 45 min, after which the collagen sheet was teased from the glass surface. In rapid succession, the ammonia solution was removed, the membrane washed twice in distilled water, and then serially rinsed with increasing concentrations of ethanol up to 70%. After storing in 70% ethanol for at least 1 wk, collagen disks were cut, using a sharpened 10-mm cork borer. These collagen disks were submerged for 5 min in 2.5% glutaraldehyde, washed in water, and attached via a collagen gluing method (13) to the roughened base of polycarbonate dishes.

Polycarbonate dishes were made from 20-mm inner diameter, 25-mm outer diameter tubing cut in 6-mm lengths, to which a solid 1-mm thick polycarbonate disk was glued. Drilling a 5-mm hole with 45° beveled edges in the center of the disk provided the chamber (0.196 $cm^2$) (see Fig. 1). The bottom of this chamber was formed by a collagen membrane supporting the T84 monolayer. The assembled dish was exposed to ammonia fumes for 5 min, immersed in 2.5% glutaraldehyde for 30 min, and stored in 70% ethanol. T84 cells were plated at 4 $\times 10^5$ cells/0.196 $cm^2$ (Fig. 1). Rings were suspended to allow basolateral access to media. Cells were also similarly plated on 12-mm glass coverslips.

## *Electrophysiologic studies*

Transepithelial resistance and solute flux were measured in modified Ussing chambers adapted for cultured epithelial monolayers, as previously described (11, 12). The sieving characteristics of the monolayer were examined by performing unidirectional flux studies in modified Ussing chambers with radiolabeled extracellular markers (mannitol 3.6

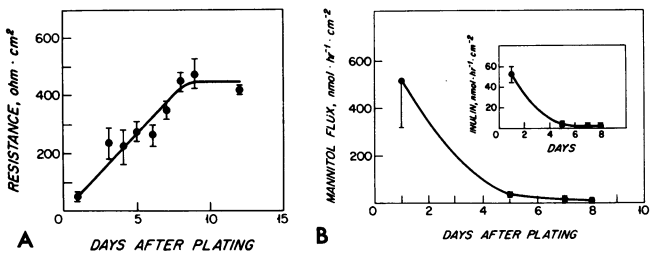


*Figure 2.* Monolayers form tight barriers 7 d after being plated at confluent density on the modified, filter-free, transparent supports. (*A*) Development of resistance. (*B*) Restriction of transepithelial flux of the inert hydrophilic solutes mannitol (3.6 Å) and inulin (11.5 Å).

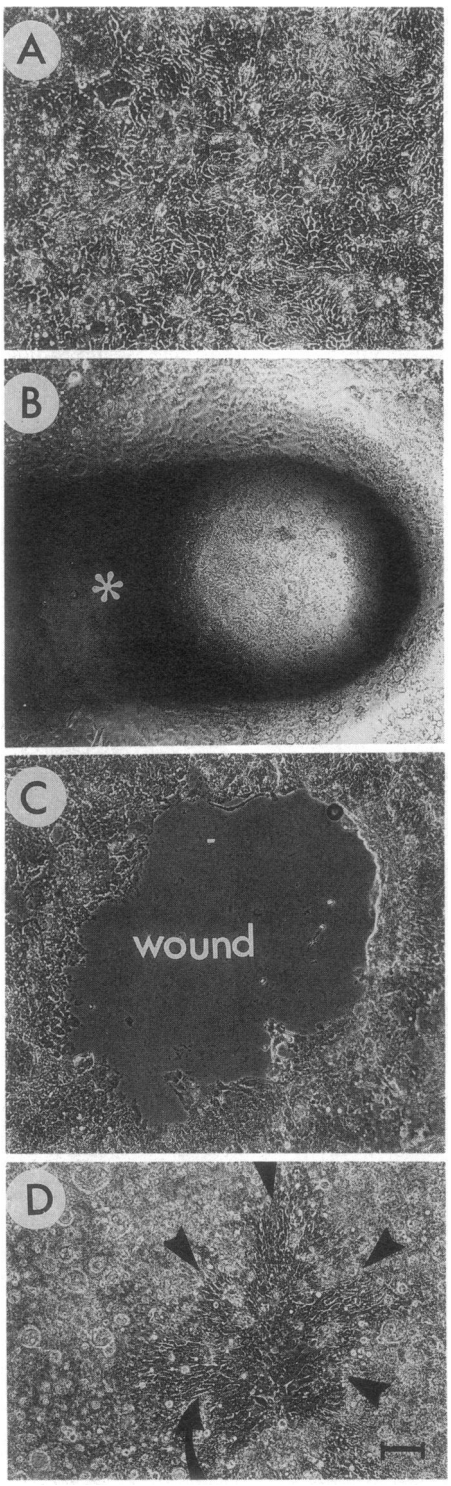


*Figure 3.* En face phase imaging of living monolayers on modified, filter-free, translucent permeable supports before (*A*), during (*B*) immediately after (*C*), and 20 h after (*D*) wounding. The micropipette (*B**) can be lowered to just touch the apical surface of the monolayer, and a disk of cells can then be removed by gentle suction without perturbation of the underlying matrix. The resulting wound (*C*) closes (*D, arrowheads*) by restitution (see text) in which cells shouldering the wound migrate to close it. The orientation of migrating cells into the wound edge can still be appreciated at 20 h (*arrow*). Note that the area of spread cells incorporates numerous cell widths. Thus, it is likely that cells immediately bordering the wound not only spread, but that this spreading phenomenon extends radially from the wound until closure is complete. Bar, ~ 100 $\mu$m.

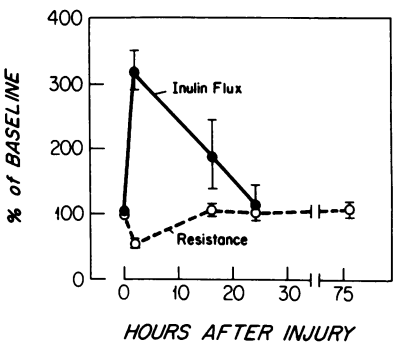


*Figure 4.* Recovery of T84 monolayer barrier function due to the restitution event shown in Fig. 3. After injury, the resistance to passive ion flow abruptly decreases and gradually returns to baseline after 18 h. This is accompanied by a parallel postwound rise in flux of mannitol and inulin which similarly return to baseline values. The mean baseline value for resistance and inulin flux in these experiments was 440 ohm · $cm^2$, and 1.3 nmol · $h^{-1}$ · $cm^{-2}$.

Å, inulin 11.5 Å), as described previously (10). Serial measurements of electrical parameters in monolayers under sterile conditions were achieved in a sterile chamber device, as previously described (15).

### *Wounding*

Wounds were made in monolayers by micropipettes (beveled tip diameter 0.5–0.6 mm) controlled by a micromanipulator (model 5170; Eppendorf Inc., Fremont, CA). The pipette was brought to the epithelial surface and a disc of epithelium removed by suction, without disturbing the underlying matrix.

### *Morphologic studies of living cells*

T84 monolayers on translucent collagen membrane supports and coverslips were visualized by phase or differential interference contrast microscopy (DIC) (Axiovert 35 M microscope; Zeiss, Oberkochen, Germany). Images of motile cells in the resealing monolayer were taken with a video camera (SIT; Hamamatsu Corp., Bridgewater, NJ; or Sanyo CCD) and analyzed (DVS-3000; Hamamatsu Corp.), recorded, and printed (Mitsubishi video cassette recorder and printer). Monolayers on membrane supports were visualized by placing the polycarbonate ring into a petri dish with a glass coverslip bottom (Fig. 1). The image analyzing system was used to calculate distances migrated by T84 cells following injury.

### *Immunofluorescent localization of actin, myosin II, villin, and fodrin in motile T84 cells*

*Actin.* This was performed using rhodamine-labeled phalloidin (Molecular Probes Inc., Eugene, OR). In the period after wounding, the resealing monolayer was rinsed in PBS, fixed for 10–15 min at room temperature in 3.7% formaldehyde, rinsed again in PBS, permeabilized for 10 min in −20°C acetone, air dried, stained with rhodamine-labeled phalloidin for 30 min at room temperature in the dark, rinsed twice in PBS, and mounted on microscopic slides in a PBS-glycerol-*p*-phenylenediamine solution (1:1:0.01) to preserve fluorescence. Cells were examined and photographed, as outlined above.

*Myosin I, myosin II, villin, and fodrin.* Resealing T84 monolayers were washed in PBS, fixed in 3.7% formaldehyde, and again rinsed in PBS. All antibodies were diluted with PBS containing 0.2% gelatin. For myosin and villin staining, cells were permeabilized in −20°C acetone for 10 min. To localize fodrin, T84 cells were permeabilized in 0.1% Triton X-100. All primary antibodies were incubated for 60 min at 20°C. (*a*) Myosin II (1:25 dilution): rabbit IgG against human nonmuscle myosin II recognizes nonmuscle myosin II as a single band on Western blots (Biomedical Technologies, Inc., Stoughton, MA). (*b*) Villin (1:100 dilution): purified IgG kappa monoclonal characterized by Dudouet et al. (16). This antibody recognizes villin in human intestinal epithelia as a single band on Western blots (Amac, Inc., Westbrook, ME). (*c*) Fodrin (1:200 dilution): this rabbit IgG antihuman brain spectrin has been characterized, and predominantly recognizes

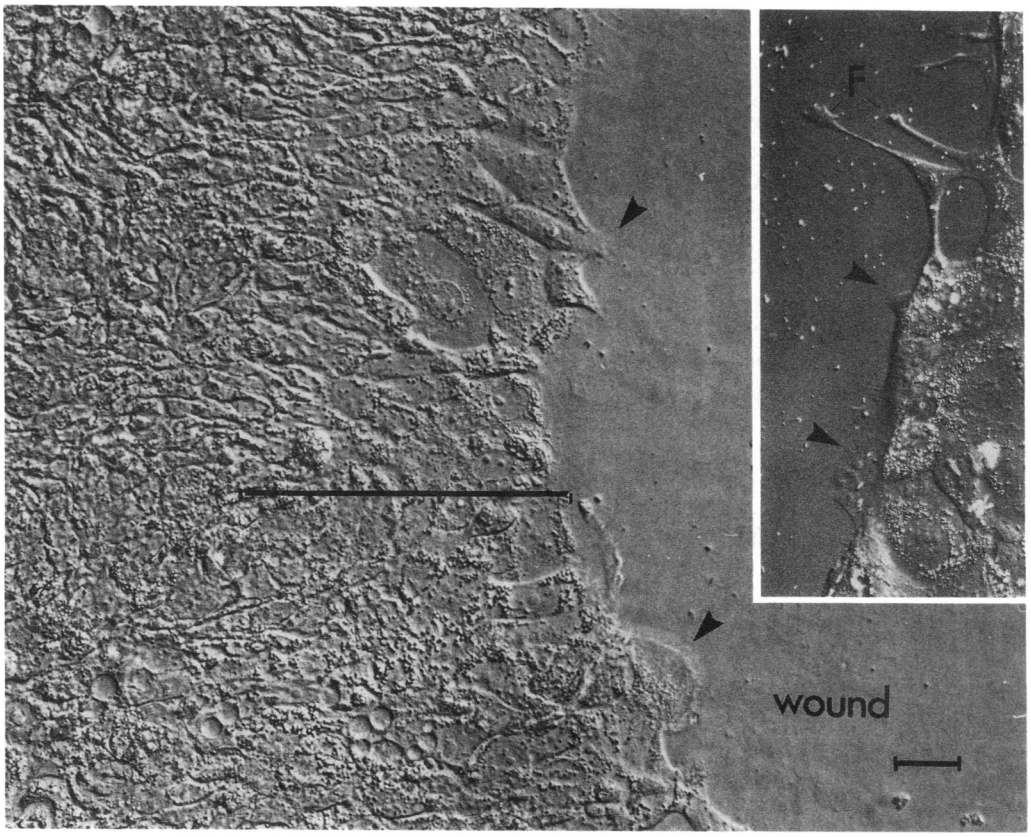


*Figure 5.* Photomicrograph (DIC) of the leading edge of a resealing monolayer. Epithelial cells shouldering the wound markedly change phenotype (within 1-h postwounding) as they migrate into the wound site. Images show motile spread epithelial cells shouldering the wound extending lamellipodia-like projections (*arrowheads*) and filopodia (*F*) (*inset*) over the denuded matrix. Cells that are several cell positions removed from the wound flatten, spread, and realign radially to the wound edge (*bracket*). Bar, ~ 100 μm.

the fodrin alpha subunit (17) (a gift from Dr. Jon Morrow, Yale University). Myosin I staining was accomplished using affinity-purified rabbit polyclonal antibody raised against avian enterocyte brush border 110 kD myosin I, which also identifies human myosin I (18) (gift of Dr. Paul Matsudaira, Whitehead Institute, Boston, MA). After incubation with primary antibodies, monolayers were washed and incubated with fluorescein-conjugated secondary antibodies. For myosin II and fodrin staining, fluorescein-conjugated goat anti-rabbit IgG was used (Organon Teknika Corp., West Chester, PA). The secondary antibody for villin was fluorescein-conjugated goat anti-mouse IgG (Boehringer-Mannheim Biochemicals, Indianapolis, IN). Monolayers were mounted as described for actin staining. Negative controls consisted of preimmune sera or staining where the primary antibody was not used.

### *Electron microscopy*

T84 monolayers were fixed for ultrastructural studies by submersion in 2% glutaraldehyde in 0.1 M Na cacodylate buffer. Subsequent processing was as previously described (8, 10).

### *Statistical analysis*

Data are presented as mean±SE. Significance is determined by Student's *t* test.

## Results

*Characterization of monolayers grown on filter-free translucent collagen.* T84 monolayers grown on the translucent collagen membranes can be imaged with clarity, and consist of a sheet of polarized columnar cells adjoined by junctional elements. Monolayers grown on this biological support mounted a substantial transepithelial resistance which reached a steady state 7–10 d after plating at ~ 450 ohm · $cm^2$ (Fig. 2 *A*). Paralleling the increase in resistance, there was a substantial restriction to permeation by the inert paracellular solutes mannitol (519±207 to 54±7 nmol · $h^{-1}$ · $cm^{-2}$) and inulin (10.8±0.7 to 1.3±0.4 nmol · $h^{-1}$ · $cm^{-2}$) by 7 d after plating (Fig. 2 *B*).

*Restitution of T84 monolayers after wounding.* As shown in Fig. 3, beveled micropipettes with 0.5-mm tips could be used to produce wounds by removing, with suction, a disk of epithelial cells from the monolayer. After injury, cells adjoining the wound flatten, spread, and migrate into the wound. Accompanying this active migration, cells surrounding the wound show varying degrees of flattening and spreading. Within 20 h the wound was closed (Fig. 3 *D*). Since T84 cells have long doubling times (confluency not reached until 7 d after a 1:2 split), the time course of the above closure response suggested that it was in large part due to flattening and migration of existing cells (i.e., "restitution"), rather than due to proliferation. Experiments with irradiated cells corroborated this. 3,000 rad, a dose that we found maximally reduced [$^3$H]thymidine incorporation into T84 cells, did not affect the ability of subsequently wounded monolayers to morphologically close in an identical fashion to that shown in Fig. 3. Additional irradiation experiments revealed that the time course of postwound electrical resealing after inhibition of proliferation was not delayed, as compared with that of control monolayers (data not shown). As assessed by phase microscopy in Fig. 3 *D*, migrated cells and their adjoining spread cells, filling the site of the wound after 20 h, occupy a discrete lower focal plane (i.e., flattened). This is in contrast to cells distant from the wound that have indistinct borders due to their columnar shape. Also, cells that have migrated into the wound are oriented perpendicular to the original edge of the wound (Fig. 3 *D*).

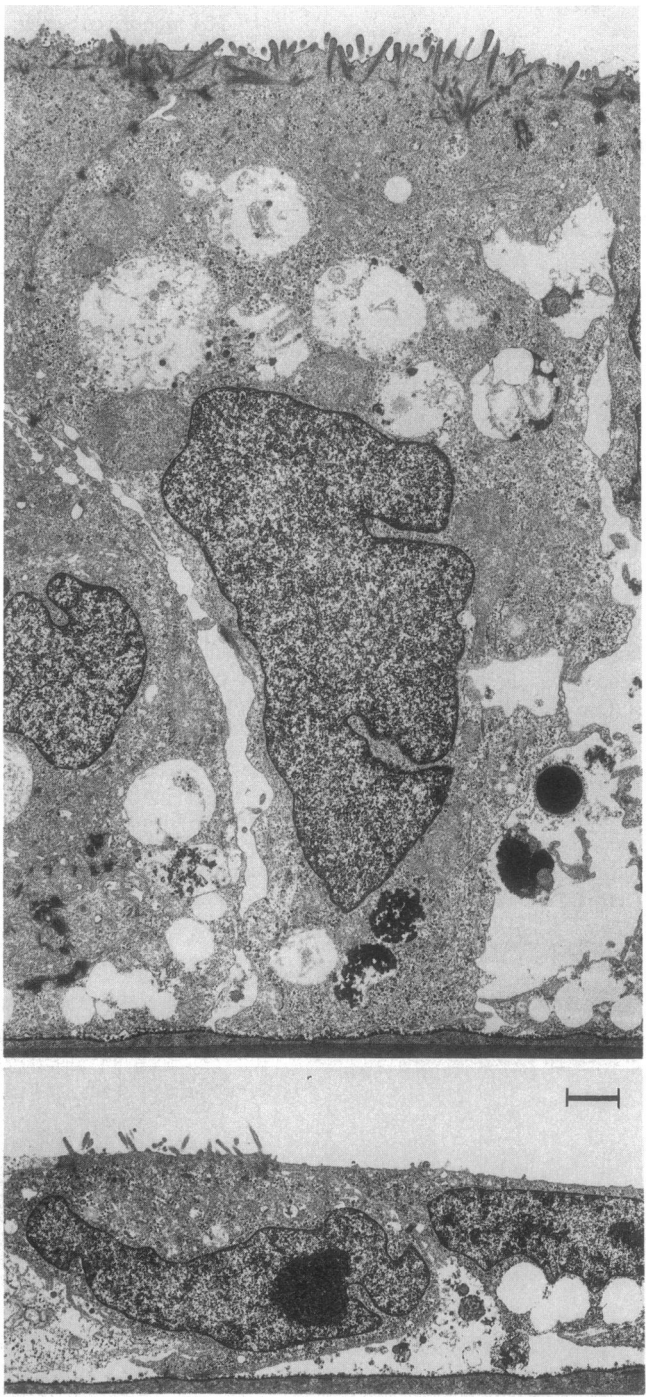

*Figure 6.* Electron micrographs obtained from wounded, resealed monolayer. (*Top*) Distant from the wound site, the usual columnar polarized phenotype of T84 cells is observed. (*Bottom*) As a result of restitution, the spread cells covering the wound (analogous to the area indicated by arrows in Fig. 3 *D*) are foreshortened, although junctions have resealed (18 h postinjury) Bar, ~ 1 μm.

As an additional approach to verify that wound closure in our system is due to cell migration, we measured the nuclear density per unit area in wounded and nonwounded sites. Nuclear density was assessed in hematoxylin stained monolayers. After reepithelialization, wounded areas had 108±8 nuclei per high power field, as opposed to columnar areas distant from

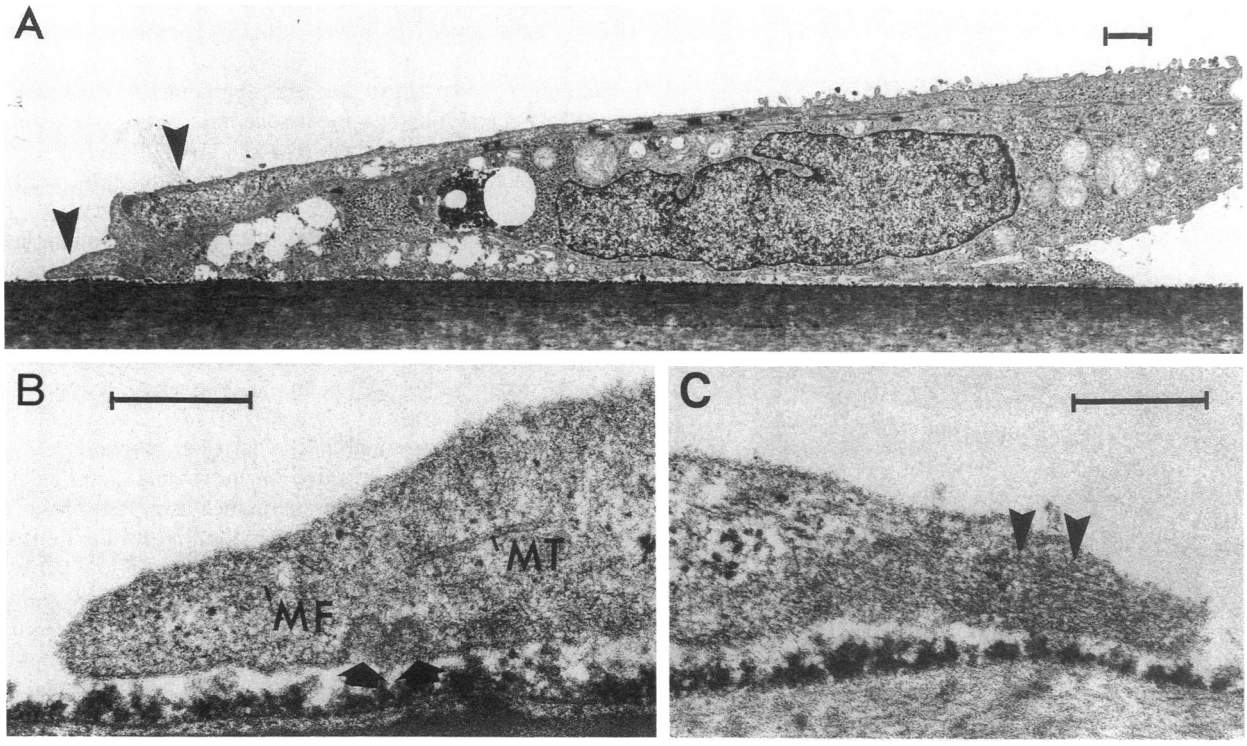


*Figure 7.* Electron micrographs of the leading edge (lamellipodia) of T84 cells migrating into wound. (*A*) Low magnification showing spread configuration. Microvilli are missing from the leading edge (*arrowhead*). (*B*) Higher magnification of the leading edge shown in *A*. The lamellipodium lacks organelles, but is enriched in cytoskeletal elements, including microfilaments (*MF*) and microtubules (*MT*). Coated pit-like structures (*arrowheads*) are also seen at the leading edge. (*C*) At the leading edge occasional dense microfilament aggregates are seen, (*arrowheads*) consistent with F actin microspikes (see Fig. 9). Bars, ~ 1 μm.

wounds that had a corresponding value roughly three times greater (360±10; $P < 0.001$). Such data quantitatively indicate that cell volume is redistributed into a flattened phenotype as cells migrated into the wound.

As shown in Fig. 4, wounds made in a controlled fashion elicited an immediate 51±3% decrease in resistance, and an immediate 320±31% increase in inulin flux. These quantitative measures of wound size returned to baseline within 18–24 h after wounding (100±14 and 111±34% of baseline value for resistance and inulin flux, respectively, at 24 h). Thus, the time course of functional recovery parallels morphologically defined restitution shown in Fig. 3.

In Fig. 5, cells on the edge of the wound undergo marked phenotypic changes that can be detected within 1 h after wounding. First, cells within several cell positions from the wound reorient such that their long axis is toward the wound (also seen in Fig. 3 *D* at time of closure). Cells shouldering the wound extend broad lamellipodia-like, and narrow filopodia-like cytoplasmic protrusions into the wound as they become markedly flattened. Moreover, as mentioned above, cells several rows adjoining the migrating front also flatten and spread to varying degrees, depending on their position relative to the wound. Thus, cells within the second row adjoining the wound are more spread, compared with those six rows away. The effect of such migration-related flattening on the ability of cells to cover surface area can be readily appreciated by comparing the crossdimensions of the flattened cells adjacent to the wound to those of the columnar cells distant from the wound in Fig. 5. Similar cell migration and spreading in response to wounding has been observed in other epithelia such as the retinal pigment epithelial cells maintained in organ culture (19). Sequential imaging revealed that T84 cells migrated into the wound at a rate of 6.6±1.5 $\mu m \cdot h^{-1}$, nearly the equivalent of one cell position per h (diameter of columnar polarized cells is ~ 8–10 μm).

*Ultrastructure of restitution.* T84 cells 50–100 cell positions removed from the wound site maintained the previously described (8, 10) normal phenotype: columnar polarized cells with scattered supranuclear vacuoles and rudimentary brush border (Fig. 6, *top*). In contrast, cells which migrated to close the wound, as shown in the en face image of unfixed monolayers in Fig. 3 *D*, were substantially flatter due to spreading. These flattened cells displayed less evidence of polarity (Fig. 6, *bottom*), although intercellular junctions were present at the basolateral/apical membrane transition site (not shown).

During the process of wound closure, the cytoplasmic protrusions at the migrating front (seen in Fig. 5) were characterized by exclusion of organelles, presumably due to the dense accumulation of cytoskeletal elements (Fig. 7, *A* and *B*). Cross sections through these sites showed microfilaments accumulated in bundled arrays that were often most dense at the interface of these lamellipodia-like processes with the underlying matrix (Fig. 7, *B* and *C*). Such extensions typically display isolated microtubules or collections of microtubules arranged parallel to the direction of migration (Fig. 7, *B* and *C*). Coated pit-like elements, characteristic of receptor-mediated endocytosis (20), were also enriched at such sites. Occasional sections through lamellipodia-like cytoplasmic protrusions revealed par-

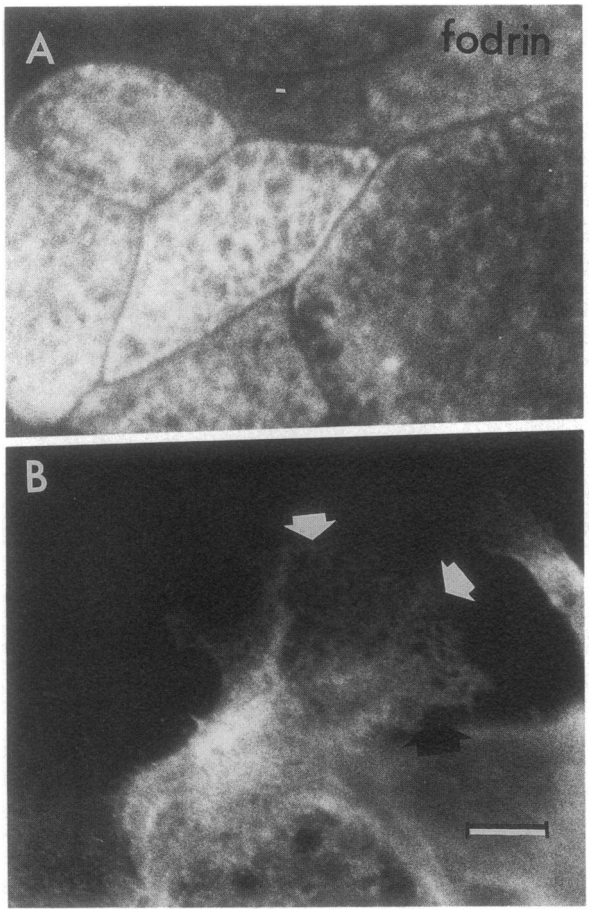


*Figure 8.* Immunofluorescent images of fodrin in T84 cells. (*A*) At sites distant from wounds, columnar T84 cells show staining of fodrin in a diffuse subcortical distribution. (*B*) In motile cells this pattern of staining is also expressed in lamellipodia (*arrowhead*). Bar, ~ 5 μm.

ticularly dense microfilament arrays within a narrow extension of the leading edge. These latter sites may correspond to the F actin microspikes described below.

*Reorganization of epithelial fodrin, F actin, myosin II, myosin I, and villin at the migrating front during restitution.* Although the imaging chamber is ideal in allowing combined functional and structural studies of the restitution process in the living state, fluorescence localization of cytoskeletal elements requires fixation, and we found substantial background fluorescence from the transparent support. Subsequent studies of wounds identically produced on glass revealed, as will be shown below, that the restitution phenotype was faithfully recapitulated, thus permitting immunofluorescence studies in this system. However, there did exist a substantial difference in the rate of T84 cell motility on glass vs Type I collagen membrane (mean rate of migration of cells at leading edge = 1.6 vs 6.6 $\mu m\ h^{-1}$ for glass vs permeable collagen support).

Fodrin, a nonerythrocyte spectrin-like molecule key in submembranous cytoskeletal organization (21), displayed a diffuse submembranous cytoskeletal organization with reticular distribution throughout lamellipodia-like protrusions, just as occurs in association with the plasma membrane of unperturbed T84 cells (Fig. 8). Since cell motility is thought to require force-based cytoskeletal interactions, we next examined F actin distribution at the migrating front. In T84 cells from unperturbed monolayers (Fig. 9, *A* and *B*) F actin is organized into four main compartments: (*a*) a prominent apical perijunctional ring; (*b*) fine apical deposits representing cytoskeletal cores of the microvilli; (*c*) a fine basolateral F actin cortex; and (*d*) scattered dense basal fibers representative of stress fibers. Marked F actin redistribution occurs within migrating cells shouldering wounds within 1–2 h (Fig. 9 *C*) and continues during restitution until closure. At the edge of the wound, lamellipodia-like protrusions are characterized by a dense F actin arc that extends across the base of the protrusions and parallels the wound's edge (Fig. 9 *D*). Within the lamellipodia are long (several micrometers), fine, F actin cables arranged perpendicular to the wound edge, and at the leading edge are brightly labeled F actin microspikes (~ 1 μm) (Fig. 9 *D*). Comparable F actin cables extend the length of the narrower filopodia.

To generate the force required for movement, actin putatively interacts with mechanoproteins such as myosin. In unperturbed monolayers, myosin II is predominantly distributed in two compartments at the light microscopic level (Fig. 10): as a perijunctional ring (*A*), and as basal stress fibers which stain with a regular periodicity (*B*). Within 3 h after injury, myosin II also extends as fibers into the basal regions of lamellipodia and filopodia-like protrusions. By 6 h after wounding, lamellipodia display fibers that stain for myosin II with a periodicity which suggests early formation of stress fibers (Fig. 10). Myosin II is predominantly localized to the basal and mid zones of lamellipodia, with occasional extension into the migrating front in the region of microspikes. In contrast to myosin II, myosin I is localized throughout lamellipodia- and filopodia-like protrusions as small dot-like plaques (Fig. 11). In several protrusions it appeared that fine dot-like myosin I signals lined up in parallel to the axis of migration. Myosin I staining occurred throughout lamellipodial protrusions but was not especially enriched at the leading edge (Fig. 11). Scattered, highly intense myosin I signal appearing as larger plaques was present in a subset of lamellipodia- and filopodia-like protrusions. In undisturbed polarized cells distal to the wound site, myosin I displayed prominent perinuclear and membrane localization (Fig. 11).

Lastly, villin, an epithelial specific F actin bundling/severing protein, was largely restricted to the brush border of T84 cells distant to wound sites as it is in natural enterocytes, although some faint basolateral staining was present (Fig. 12 *A*) (22). However, at the wound site, within 2–3 h after injury, villin was redistributed and found multifocally in the longitudinal fibers extending into lamellipodia (Fig. 12 *B*), in arcs at the base of lamellipodia (Fig. 12 *C*), and focally at sites suggesting colocalization with F-actin rich microspikes (Fig. 12 *D*). A prominent feature of villin distribution in lamellipodia-like projections, in contrast to F actin, myosin II, myosin I, or fodrin, was the marked variability and nonuniformity of its appearance in the above sites. This would suggest its role in remodeling of F actin during the constant ebb and flow of cytoplasmic protrusion, as discussed below.

## Discussion

We describe a cell culture model of intestinal epithelial wound closure that incorporates a translucent biological support, and

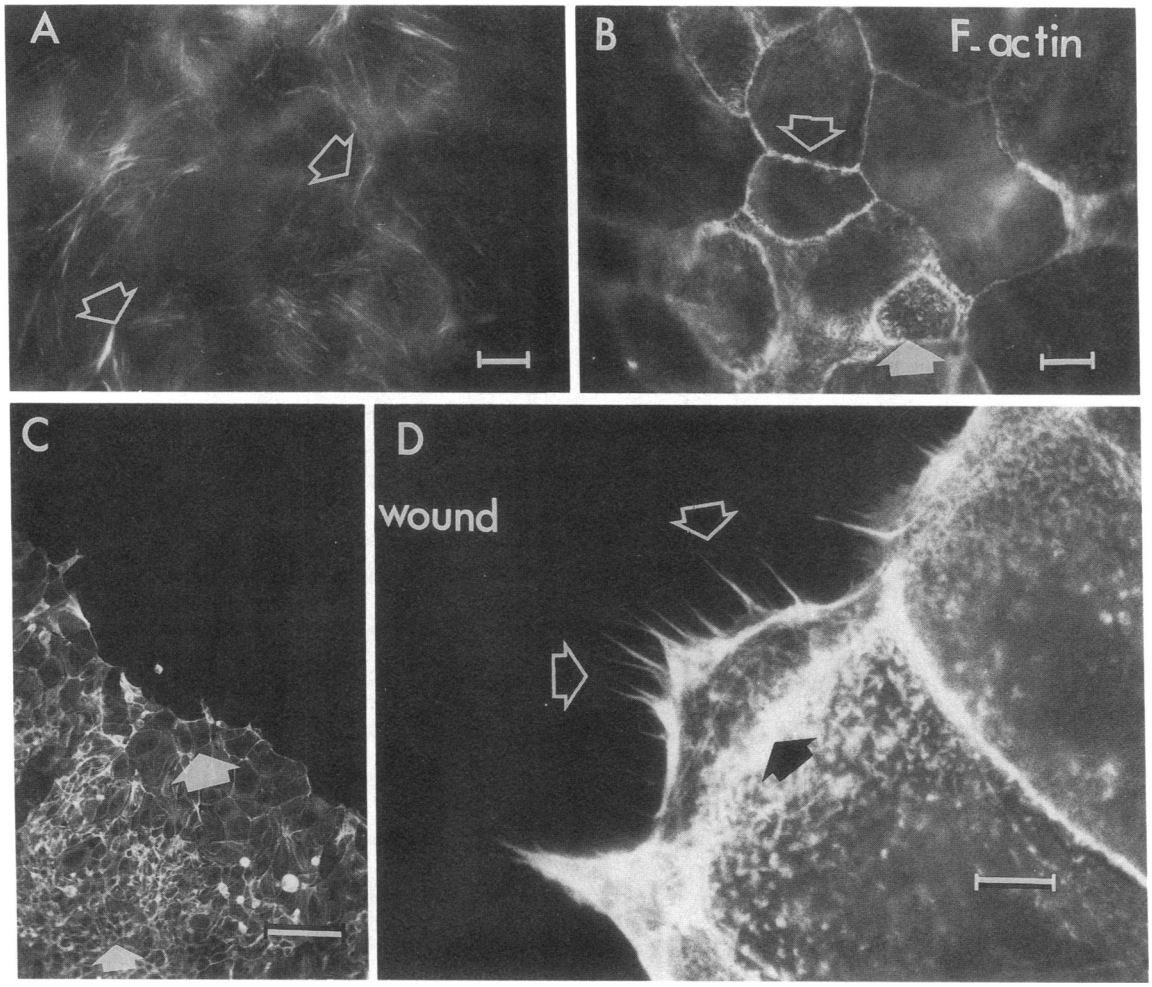


*Figure 9.* Fluorescence images localizing F actin (rhodamine–phalloidin) in T84 cells. (*A*) Basal plane of focus in columnar T84 cells at site distant from wound repair. Scattered F actin filaments (*arrows*) are seen. (*B*) Apical plane of focus in columnar T84 cells at site distant from wound repair. Faint F actin spicules representative of microvilli (*solid arrows*) are seen surrounded by the prominent F actin perijunctional ring (*open arrow*). (*C*) Low magnification of F actin distribution at wound's edge showing spreading of multiple cell layers bordering the wound. At the leading edge within 2 h of wounding the shape of T84 cells changes from narrow columnar (*small arrow*) to broad flattened (*large arrow*). The apical F actin ring of the tall columnar cells in the lower left corner appears out of focus since it now occupies a higher focal plane than the spread cells at the wound's margin. Lamellipodia and filopodia-like projections can be seen along the advancing edge. (*D*) At higher magnification, lamellipodia projecting from the leading edge display a prominent F actin arc at their base (*black arrow*), fine F actin filaments within them, and F actin labeled microspikes in the front (*open arrows*). Bars, ~ 5 μm for *A*, *B*, and *D*, and ~ 50 μm for *C*.

that recapitulates the essential features of restitution (1, 2) in natural intestinal epithelia. For example, epithelial lamellipodia-like extensions are known to underlie restitution in natural epithelia (1, 2), but the complex geometry of these systems greatly restricts detailed analysis of such structures and events. In contrast, the model reported here enables one to measure functional parameters of resealing, while simultaneously imaging cell shape change and migration by phase or Nomarski optics. Cell migration, an essential feature of restitution, has been investigated in diverse cell types which include fibroblasts, macrophages, dictyostelium, ameba, fish keratocytes, and retinal pigment epithelial cells (7, 19, 23, 24, 25). We find that intestinal epithelial cell migration subsequent to wounding shares many features common to cell migration in such simple (and nontransformed) systems. For example, fibroblasts, macrophages, and retinal pigment epithelial cells also move by extending broad lamellipodia in the direction of movement (7, 19). As shown here, such lamellipodia-like protrusions are also clearly imaged in migrating intestinal epithelial cells. Such lamellipodia, in combination with cell flattening and spreading, represent the initial events in covering the denuded surface area. Ultrastructural analysis showed epithelial lamellipodia to include dense collections of microfilaments running perpendicular to the wound edge, with focal dense microfilament collections at the most anterior portion of lamellipodia. Similar microfilament bundles have been identified in other migrating epithelial cells such as migrating retinal pigment epithelial cells maintained in organ cultures (19).

Examination of the anatomy of specific cytoskeletal elements in migrating intestinal epithelial cells during restitution defined not only similarities to events in migrating nonepithelial cells, but also interesting differences. As discussed below, such differences may be of substantial importance since epithelial cells display some unique cytoskeletal elements not present

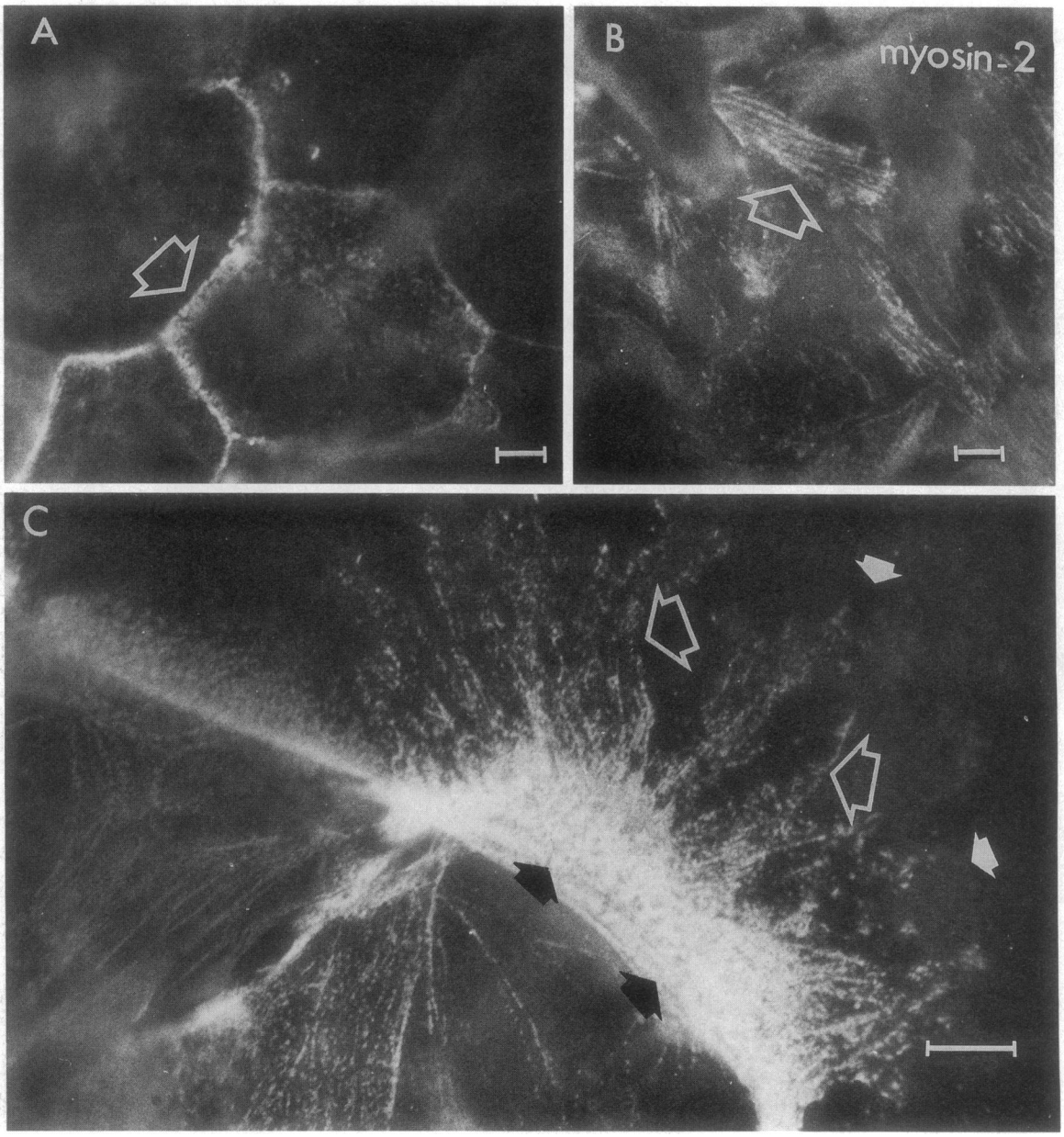


*Figure 10.* Immunofluorescent images of myosin II in restituting T84 cells. (*A*) Apical plane of focus in columnar T84 cells at site distant from wound. Myosin II is seen as a perijunctional ring. (*B*) Basal plane of focus in cells distant from the wound reveals periodic staining in basal stress fibers. (*C*) In migrating cells, myosin II filaments extend, in an arc-like fashion, across the lamellipodia base (*black arrows*), and also radiate into the lamellipodia (*open arrows*), with occasional extension close to the leading edge (*solid arrows*). Bars, ~ 5 μm.

in fibroblasts, macrophages, or amebas. The actin cytoskeleton has been implicated as an important element required for cell locomotion in diverse cell types, including neutrophils, retinal pigment epithelial cells, embryonic chicken gizzard cells, neurons, fish keratocytes, and the slime mold dictyostelium. These cells reorganize F actin at the leading edge, which appears to support lamellipodia or growth cones of neurites (19, 26–31). The exact mechanism of actin polymerization/depolymerization, and the contribution of these events to lamellipodial extrusion, is, however, not clear. This process is likely to be crucial in force generation, and is thought to mechanistically mediate cell locomotion (7, 25, 31, 32). Models proposed to explain the contribution of F actin to lamellipodial protrusion, and therefore cell locomotion, include treadmilling and the nucleation release model. Treadmilling, a process by which actin monomers are added to F actin filaments at the advancing edge with depolymerization proximally, provides the force for forward extension of lamellipodia (24). Theriot and Mitchison have proposed a nucleation release model for actin filament dynamics in lamellipodia of rapidly migrating fish keratocytes (25). According to their model, short randomly oriented and rapidly exchanging actin filaments exist in lamellipodia that advance by a greater degree of actin polymerization at the cell margin than the rear. However, no unified theory to explain

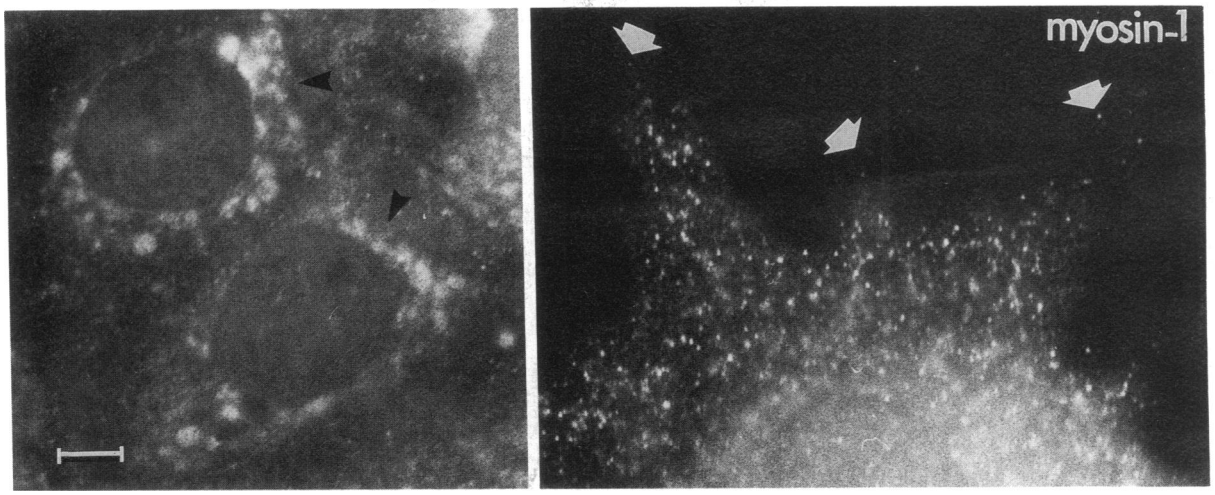


*Figure 11.* Immunofluorescent images of myosin I in normal nonmigrating T84 cells and in lamellipodia-like extensions of migrating T84 cells. (*Left*) In columnar cells removed from the wound, myosin I has a perinuclear and presumably membrane-associated pattern as has been described in some other cell types. (*Right*) Throughout lamellipodia, myosin I is distributed as dot-like plaques. Occasionally, faint linearity is noted. Discrete staining can be seen at the leading edge (*arrows*), but myosin I is not concentrated here. Bar, ~ 2 μm.

actin dynamics in lamellipodia of mammalian epithelial or nonepithelial cells exists. F actin within lamellipodia of nonepithelial cells may move toward the cell interior during migration, forming arcs across the base of lamellipodia which then may be swept rearward as motility proceeds (see reference 7 for review). Arcs similar to those observed in our T84 cell model are seen in intestinal epithelial cells, and like those in fibroblasts, they also display myosin II periodicity. Comparable fibers with myosin II periodicity also extended into the lamellipodia-like protrusions. Such fibers are predominantly localized to the basal regions of lamellipodia, with an occasional extension to the advancing front of motile T84 cells in regions of actin microspikes. It has recently been suggested that the mechano-proteins with which actin interacts to generate contractile force at the leading edge of migrating cells are members of a new myosin family (myosin I), which are largely membrane associated (33). Evidence for this originated in ameboid cells using recombination mutants lacking functional myosin II (34), and in microinjection studies using myosin II antibody (35) or antisense RNA (36). When functional myosin II was so depleted, it was found that these cells still exhibited directed motility, although minor characteristics of the motility pattern were altered (34–36). Such motility was subsequently suggested to be myosin I based (33). We show that similar to studies of the slime mold dictyostelium (33), myosin I proteins are expressed in restituting intestinal epithelial cells at the leading edge. However, in contrast to those studies, we find no evidence of specific enrichment of myosin I at the leading edge of lamellipodia.

As alluded to above, while several features of motility are shared between T84 cells and nonepithelial cells, striking differences also exist. One striking difference is the appearance of villin in lamellipodia-like extensions at the leading edge. Villin, a 95-kD epithelial-specific cytoskeletal protein which, depending on intracellular calcium concentration, may serve either as an F actin bundling or severing protein (22). Villin has a restricted localization in confluent epithelial sheets of columnar cells including T84 cells. It is chiefly associated with the microvillus core bundle of F actin, although lesser association with actin distributed on the lateral membrane also occurs (22). Recent studies have shown that when villin is transfected into fibroblasts, there is dramatic lengthening of F actin bundles projecting from the cell surface (37). Such results were interpreted as indicating villin-induced formation of nascent brush borders in a nonepithelial cell type. As expected, we find that T84 cells also express brush border villin, as do other intestinal epithelial cell lines such as CaCo-2 (38). However, in restituting cells, we find villin also expressed in lamellipodia. A striking characteristic of villin distribution in lamellipodia, as opposed to that of F actin, fodrin, myosin II, or myosin I, is the marked nonuniformity of the former, a result that may suggest a role of villin in the dynamic F actin severing/bundling cascade likely to occur with movement of lamellipodia. Such findings suggest that epithelial cell locomotion during restitution may show unique differences from locomotion in nonepithelial cell types. The incorporation of epithelial-specific cytoskeletal proteins such as villin into the cascade of events that result in functionally and morphologically defined wound closure may be necessary. Therefore, future studies using microinjection of antibodies or antisense RNA to villin and/or transfections of intestinal epithelia with villin mutants are needed to clarify the speculative functional role of this protein in restitution.

Lamellipodial extrusion, cell spreading, and locomotion is a complex phenomenon likely to be dependent on multiple coordinate events that include dynamic actin restructuring, force transduction by mechanoproteins such as members of the myosin I and II family, and cell–matrix interactions. Cell–matrix interactions have been observed in lamellipodia of migrating epithelial (19) and nonepithelial cells (39) at sites termed focal contacts or focal adhesion plaques. Actin microfilaments in lamellipodia are closely associated to the extracellular matrix via proteins in focal contacts that include vinculin and talin. Actin microfilaments are hypothesized to transmit force on the substratum and provide traction for the leading edge

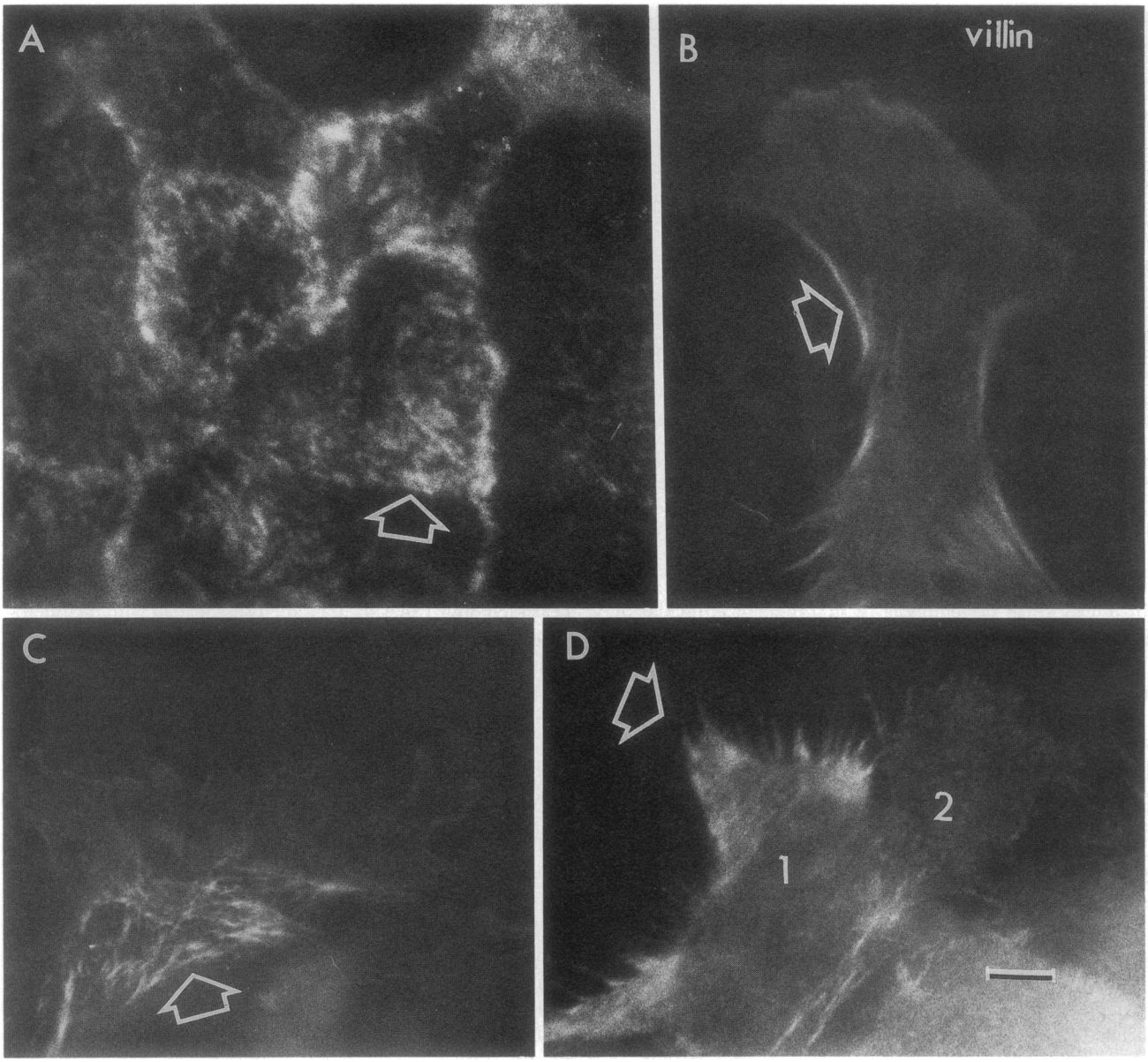


*Figure 12.* Immunofluorescence localization of the epithelial-specific F actin bundling and severing protein villin. (*A*) En face view in the plane of the apical membrane. Villin staining is shown by the arrows. At sites distant to wounds, or in intact monolayers, villin is restricted to the microvillus border as in native intestine. The appearance of a fine flocculated apical distribution is indicative of its presence in microvilli. The increased perijunctional staining density is due to the known increased density of microvilli at this site. (*B–D*) Villin staining occurs at the leading edge, but is much more variable in pattern at this site than is staining for F actin, myosin II, or fodrin. Lamellipodia can stain at the periphery (*B*), at the zone of the F actin arc (*C*), or within microspikes (*D*). As shown in *D*, substantial variability in villin staining occurs between even adjacent lamellipodia (compare lamellipodia 1 with lamellipodia 2). Bar, ~ 5 μm.

protrusion. Our studies provide a model with which such mechanistic studies can be pursued.

## Acknowledgments

We thank Drs. Mark Mooseker, John Morrow, Susan Hagen, and Paul Matsudaira for gifts of antibody and helpful comments. We thank Susan Carlson for her expert assistance with electron microscopy and photography.

This work was supported by National Institutes of Health grant DK-35932. Dr. Nusrat is supported by an individual National Research Service Award DK08409.

## References

1. Rutten, M. J., and S. Ito. 1983. Morphology and electrophysiology of guinea pig gastric mucosal repair *in vitro*. *Am. J. Physiol.* 244G:171–182.

2. Moore, R., S. Carlson, and J. L. Madara. 1989. Rapid barrier restitution in an *in vitro* model of intestinal epithelial injury. *Lab. Invest.* 60:237–244.

3. Feil, W., E. Wentzl, P. Vattay, M. Starlinger, R. Sogukoglu, and R. Schiessel. 1982. Repair of rabbit duodenal mucosa after acid injury *in vivo* and *in vitro*. *Gastroenterology.* 92:1973–1986.

4. Moore, R., S. Carlson, and J. L. Madara. 1989. Villus contraction aids repair of intestinal epithelium after injury. *Am. J. Physiol.* 257:G274–G283.

5. Bretcher, M. S. 1984. Endocytosis: relation to capping and cell locomotion. *Science (Wash. DC).* 224:681–686.

6. Conrad, P. A., M. A. Nederlof, I. M. Herman, and D. L. Taylor. 1989.

Correlated distribution of actin, myosin and microtubules at the leading edge of migratory Swiss 3T3 fibroblasts. *Cell Motil. Cytoskeleton.* 14:527–543.

7. Singer, S. J., and A. Kupfer. 1986. The directed migration of eukaryotic cells. *Annu. Rev. Cell. Biol.* 2:337–365.

8. Madara, J. L., J. Stafford, K. Dharmsathaphorn, and S. Carlson. 1987. Structural analysis of a human intestinal epithelial cell line. *Gastroenterology.* 92:1133–1145.

9. Madara, J. L., D. Barenberg, and S. Carlson. 1986. Effects of cytochalasin D on occluding junctions of intestinal absorptive cell. Further evidence that the cytoskeleton may influence paracellular permeability and junction charge selectivity. *J. Cell Biol.* 102:2125–2126.

10. Madara, J. L., and K. Dharmsathaphorn. 1985. Occluding junction structure-function relationships in a cultured epithelial monolayer. *J. Cell Biol.* 101:2124–2133.

11. Dharmsathaphorn, K., J. A. McRobert, K. G. Mandel, L. D. Tisdale, and H. Masui. 1984. A human colonic tumor cell line that maintains vectorial electrolyte transport. *Am. J. Physiol.* 246:G204–G208.

12. Dharmsathaphorn, K., and J. L. Madara. 1990. Established intestinal cell lines as model systems for electrolyte transport studies. *Methods Enzymol.* 192:354–389.

13. Steele, R. E., A. S. Preston, J. P. Johnson, and J. S. Handler. 1986. Porous-bottom dishes for culture of polarized cells. *Am. J. Physiol.* 251 (*Cell Physiol. 20*):C136–C139.

14. Cereijido, M., E. S. Robbins, W. J. Dolan, C. A. Rotunno, and D. D. Sabatini. 1978. Polarized monolayers formed by epithelial cells on a permeable and translucent support. *J. Cell Biol.* 77:853–876.

15. Hecht, G., C. Pothoulakis, J. T. LaMont, and J. L. Madara. 1988. C. difficile toxin A perturbs cytoskeletal structure and tight junction permeability of cultured human intestinal epithelial monolayers. *J. Clin. Invest.* 82:1516–1524.

16. Dudouet, B., S. Robine, C. Huet, C. Sahuquillo-Merino, L. Blair, E. Coudrier, and D. Louvard. 1987. Changes in villin synthesis and subcellular distribution during intestinal differentiation of HT29-18 clones. *J. Cell Biol.* 105:359–369.

17. Harris, A. S., J. P. Anderson, P. D. Yurchenco, L. A. D. Green, K. J. Ainger, and J. S. Morrow. 1985. Mechanisms of cytoskeletal regulation (I): functional differences correlate with antigenic dissimilarity in human brain and erythrocyte spectrin. *Biochim. Biophys. Acta.* 830:147–158.

18. Collins, K., J. R. Sellers, and P. Matsudaira. 1990. Calmodulin dissociation regulates brush border myosin I (110 KD-calmodulin) mechanochemical activity in vitro. *J. Cell Biol.* 110:1137–1147.

19. Hergott, G. J., M. Sandig, and V. I. Kalnins. 1989. Cytoskeletal organization of migrating retinal pigment epithelial cells during wound healing in organ culture. *Cell Motil. Cytoskeleton.* 13:83–93.

20. Brodsky, F. M. 1988. Living with Clathrin: its role in intracellular membrane traffic. *Science (Wash. DC).* 242:1396–1401.

21. Glenney, J. R., and P. Glenney. 1983. Fodrin is the general spectrin-like protein found in most cells whereas spectrin and the TW protein have restricted distribution. *Cell.* 34:503–512.

22. Mooseker, M. S. 1985. Organization, chemistry and assembly of the cytoskeletal apparatus of the intestinal brush border. *Annu. Rev. Cell Biol.* 1:209–241.

23. Bergmann, J. E., A. Kupfer, and S. J. Singer. 1983. Membrane insertion at the leading edge of motile fibroblasts. *Proc. Natl. Acad. Sci. USA.* 80:1367–1371.

24. Wang, Y. L. 1985. Exchange of actin subunits at the leading edge of living fibroblasts: possible role of treadmilling. *J. Cell Biol.* 101:597–602.

25. Theriot, J. A., and J. Mitchison. 1991. Actin microfilament dynamics in locomoting cells. *Nature (Lond.).* 352:126–131.

26. Condeelis, J., Hall, A., Bresnick, A., Warren, V., R. Hock, H. Bennett, and Ohihara, S. 1988. Actin polymerization and pseudopod extension during ameoboid chemotaxis. *Cell Motil. Cytoskeleton.* 10:77–90.

27. Omann, G. M., R. A. Allen, G. M. Bokoch, R. G. Painter, A. E. Traynor, and L. A. Sklar. 1987. Signal transduction and cytoskeletal activation in the neutrophil. *Physiol. Rev.* 67:285–322.

28. Kreis, T. E., B. Geiger, and J. Schlessinger. 1982. Mobility of microinjected rhodamine actin within living chicken gizzard cells determined by fluorescence photobleaching recovery. *Cell.* 29:835–845.

29. Mitchison, T. J., and M. Kirschner. 1988. Cytoskeletal dynamics and nerve growth. *Neuron.* 1:761–772.

30. Smith, S. J. 1988. Neuronal cytomechanics: the actin based motility of growth cones. *Science (Wash. DC).* 242:708–715.

31. Heath, J., and B. Holifield. 1991. Actin alone in lamellipodia. *Nature (Lond.).* 352:107–108.

32. Bretcher, M. S. Fibroblasts on the move. 1988. *J. Cell Biol.* 106:235–237.

33. Fukui, Y., T. J. Lynch, H. Brzeska, and E. D. Korn. 1989. Immunofluorescence localization of myosin I in Dictyostelium. *Nature (Lond.).* 341:328–331.

34. De-Lozanne, A., and J. A. Spudich. 1987. Disruption of the Dictyostelium myosin heavy chain gene by homologous recombination. *Science (Wash. DC).* 236:1086–1091.

35. Sinard, J., and T. D. Pollard. 1989. Microinjection into Acanthamoeba castellanii of monoclonal antibodies to myosin II slows but does not stop cell locomotion. *Cell Motil. Cytoskeleton.* 12:42–52.

36. Knecht, D. A., and W. F. Loomis. 1987. Anti-sense RNA inactivation of myosin heavy chain gene expression by homologous recombination. *Science (Wash. DC).* 236:1086–1091.

37. Friedrich, E., C. Huet, M. Arpin, and D. Louvard. 1989. Villin induces microvilli growth and actin redistribution in transfected fibroblasts. *Cell.* 59:461–475.

38. Peterson, M. D., and M. S. Mooseker. 1990. Characterization of CaCo-2 cells as a model for brush border cytoskeletal assembly. *J. Cell Biol.* 111:165a. (abstract).

39. Rinnerthaler, G., B. Geiger, and J. V. Small. 1988. Contact formation during fibroblast locomotion: involvement of membrane ruffles and microtubules. *J. Cell Biol.* 106:747–760.